Institute of Space and Aeronautical Science, University of Tokyo
Report No. 578, February 1980

Design and Performance of a Variably-Humidified Air Flow Supplying System

By

Hiroshi TSUJI, Kiyoshi MATSUI and Atsushi MAKINO

Summary: A variably-humidified air flow supplying system has been constructed for the study of combustion phenomena which are strongly affected by the concentration of water vapor contained in an oxidizer. In this system, the water-vapor concentration can be controlled in the range of $0.001 \sim 0.1$ in mole fraction at a total pressure of atmospheric; the maximum mass flow-rate of the air (excluding the water-vapor mass contained in it) is 0.17 kg/s. The air is first excessively humidified and then dehumidified so that its humidity becomes a desired value. Humidifying is made by contact of the air with the liquid water surface. Dehumidifying is achieved principally by the contact cooling method (the method in which a humid gas is dried by direct contact with a solid surface whose temperature is lower than the dew point of the gas) and supplementarily by the expansion method (the method in which a humid gas is dried by decrease of its total pressure). Design principles, detailed specifications of the apparatus, and the results of the performance tests are described.

1. INTRODUCTION

The concentration of water vapor contained in oxidizer gases strongly affects the combustion of some gases and some solids. The combustion of carbon monoxide or of solid carbon is an example. In order to investigate experimentally the effect of the water-vapor concentration on such combustions, we have constructed a variably-humidified oxidizer flow supplying system. In this system, air is used as an oxidizer; the water-vapor concentration can be controlled in a range of $0.001 \sim 0.1$ in mole fraction under a total pressure of atmospheric for a given flow rate of air. The maximum mass flow-rate of the air (excluding the water-vapor mass contained in it) is 0.17 kg/s.

Air flow supplying systems in which the air humidity is controlled are widely used in chemical engineerings. In those systems, usually, the humidity cannot be varied in wide ranges, and the air flow-rates are large. On the other hand, humidity-controlled air flow supplying apparatus made of glass tubes and glass wares (mostly used in laboratories of chemistry) supply only small flow-rates of air. And examples of the variably-humidified air flow supplying system having the air mass flow-rates of few hundreds of grams a second are seemingly few. Therefore, we report here the full details of the design and the performance of our system for the information of those investigators engaged in related fields.

2. Design of System

2.1 Design Principle

We have planned to make the humidified air either issue into the quiescent atmosphere as a free jet or flow in a combustion tunnel whose downstream end opens to the atmosphere. That is, the humidified air is to be used under atmospheric pressure or pressures slightly higher than atmospheric. The maximum mass flow-rate of the air (excluding the water-vapor mass contained in it) is chosen 0.17 kg/s because this rate suffices for small-scale, continuous combustion experiments. (For example, an air-flow velocity of 27 m/s is obtained in a tunnel of 50 cm^2 cross-sectional area at a pressure of 0.103 MPa and a temperature of 288 K.) We have intended to make the maximum water vapor concentration in the humidified air 0.1 in mole fraction and to vary the concentration by a factor of 100. Therefore, the maximum dew point of the humidified air was set 320 K, and the minimum 253 K (exactly, these correspond to the water-vapor concentration of 0.1037 and 0.0009990 in mole fraction under a total pressure of 0.1013 MPa). By the way, this range is wider than the usual range of the meteorological humidity.

2.2 The Method of Control of Humidity

Principle The air fed by the air supplying facilities in the present system has a dew point lower than 263 K. This air is first humidified to an extent that its dew point becomes higher than the desired value. The air is then dehumidified to the desired dew point.

The air is humidified by the contact with liquid water surface. Dehumidifying is achieved principally by the contact cooling method, and supplementarily by the expansion method. Here, the former means the method for gas-drying in which a humid gas is dried by direct contact with a solid surface whose temperature is lower than the dew point of the gas. The expansion method rests on the law that the dew point of a humid gas decreases with its total pressure; this method supplies a deficiency inherent in the contact cooling method that the dew point of the humid gas cannot be made lower than the temperature of the solid surface. A more detailed explanation of this expansion method is given in §A.1 of the Appendix.

Practice Figure 1 shows schematically the system in which the aforementioned

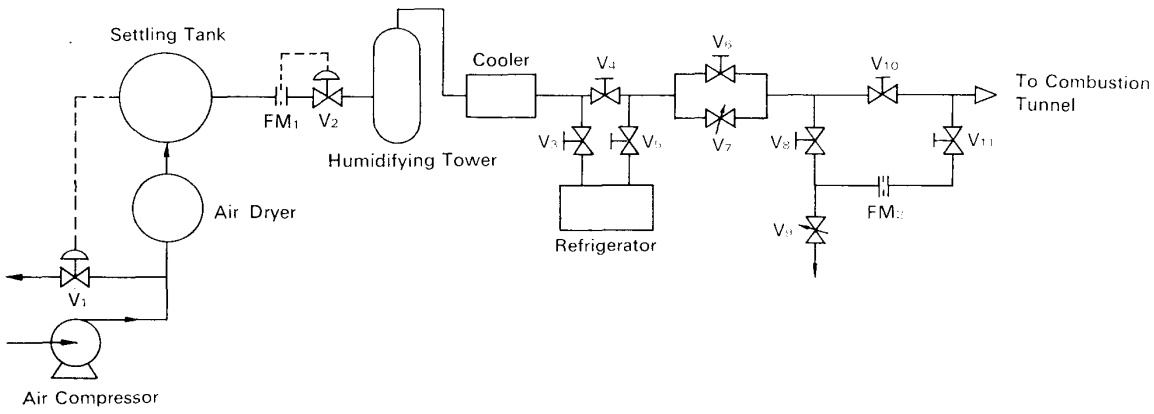

FIG. 1. Schematic flowchart of the system.

principles of humidity control are practiced. The parts upstream of the inlet of the humidifying tower are the existing facilities for supplying air flow. The air pressure upstream of the orifice flow meter FM1 and the pressure reduction through the orifice can be controlled automatically to given values.

Humidifying of the air supplied by the existing facilities is made in the humidifying tower. The air simply flows over the surface of unheated water stored in the bottom (to be lightly humidified) or flows up against a shower of either unheated water (to be moderately humidified) or heated water (to be heavily humidified).

Dehumidifying of the air by the contact cooling method is performed by either a cooler or a refrigerator. The dew points of the air at the outlets of these apparatus are regulated by variation of their cooling capacities. The cooling capacity of the cooler is varied by the change of the flow rate of its cooling water. The *hot-refrigerant-bypass* method is used for variation of the cooling capacity of the refrigerator. By this method, however, its cooling capacity can be varied only in a narrow range, and so, regulation of the air dew-point cannot be achieved for a wide range of the air flow-rate. Therefore, when the refrigerator is used, the air flow-rates passing through it are fixed at some favorable values; control of the air flow-rate is made downstream of its outlet. The expansion method is performed simply by expansion of the air with the expansion valve V7.

The final flow rate of the air is usually controlled by the valve V2 in combination with the orifice flow meter FM1. When the refrigerator is used, the final flow rate is controlled in the circuit line including FM2. In this line the air flow-rate is controlled by exhausting some of the inflowing air into the atmosphere by V9; the air flow-rate is measured with the orifice flow meter FM2. The walls of the lines downstream of the outlet of the cooler (excluding the circuit line) are heated for condensation of water vapor in the air flow to be prevented.[1)]

Table 1. Combination of Methods of Humidifying and Dehumidifying with Indication of Control of Humidity and Air Flow-Rate

Range of Dew Point K	Extent of Humidifying			Method of Dehumidifying			Air Flow-Rate Control by		Route of Air through
				Contact Cooling by		Expansion			
	Light	Moderate	Heavy	Cooler	Refrigerator		V_2	V_9	
320~309			○	○△			○		V_4 V_6 V_{10}
309~291			○	○		○△	○		V_4 V_7 V_{10}
291~276		○		○		○△	○		V_4 V_7 V_{10}
276~274	○				○△			○	V_5 V_6 V_{11}
274~253	○				○	○△		○	V_5 V_7 V_{11}

Note: The symbol ○ indicates what applies; △ indicates that the final control of the humidity is done there.

1) Heating of the wall of the circuit line is unnecessary because the dew point of the air flowing through this line is lower than the room temperature.

These practical methods of humidifying and dehumidifying are combined in several ways depending on desired air-humidity. These combinations together with indication of the apparatus for air-humidity and flow-rate control are illustrated in Table 1. The ranges of the dew point shown in this table are typical: they somewhat vary as the ambient atmospheric temperature or the cooling-water temperature changes.

2.3 *Constitution of System*

Figures 2 and 3 show the distribution diagrams of the present system; Fig. 2 includes the main lines; Fig. 3 the water-supplying and -draining lines. Specifications of the auxiliary equipments are given in Table 2, and those of the measuring apparatus in Table 3. Explanations of the main apparatus and the air supplying facilities are given in the following subsections.

Air supplying facilities Air is supplied continuously by a 116 kW, screw-type, rotary compressor (the nominal flow-rate, 0.28 kg/s at 0.69 MPa); the compressed air is dried by passage through a tower filled with silica gel. Six orifice flow meters are provided. The pressure upstream of the orifice and the flow rate can be controlled in the ranges of 0.268 ~ 0.690 MPa and $1.1\times10^{-3}\sim2.8\times10^{-1}$ kg/s. The details of these air supplying facilities are given in reference 1.

Humidifying tower The structure of the humidifying tower is illustrated in Fig. 4. Water is stored in the bottom. When the shower is needed, this water is pumped up and sprayed from the six nozzles arranged in a circle. Heating of the stored water (needed when a hot shower is used) is made by the six electric heaters plunged into the water. The output of each heater is 7 kW; these six heaters are divided into three pairs; one pair is automatically controlled (on-off control) by indication of the water

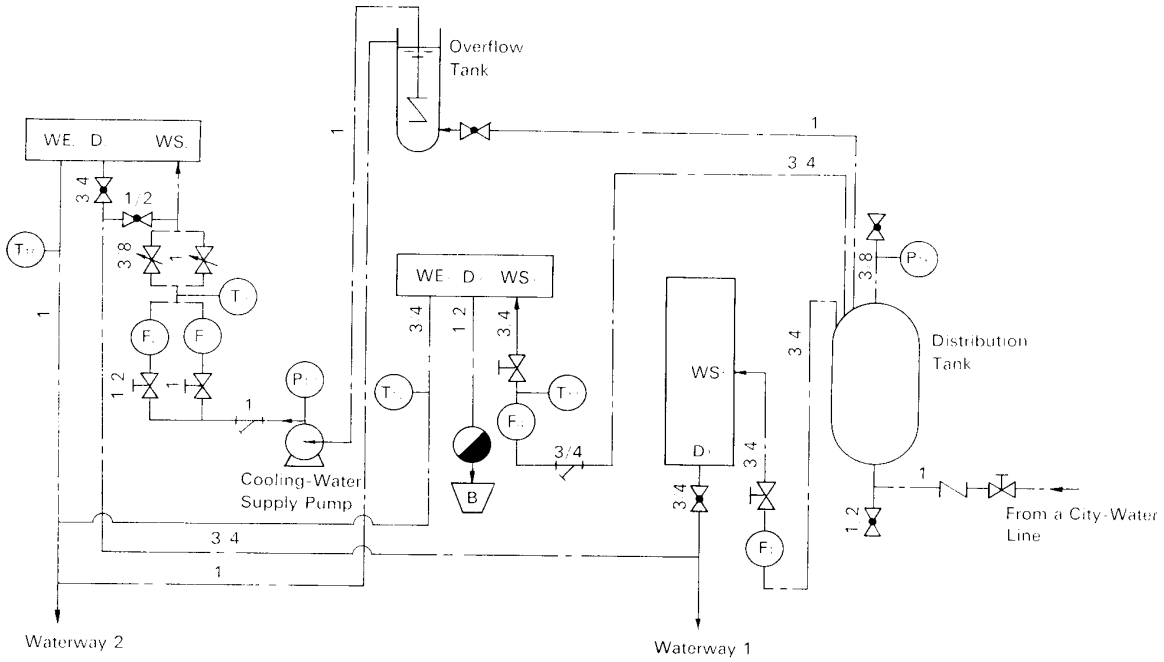

FIG. 3. Distribution diagram of the water-supplying and -draining lines of the system. (The meanings of the symbols are the same as in Fig. 2.)

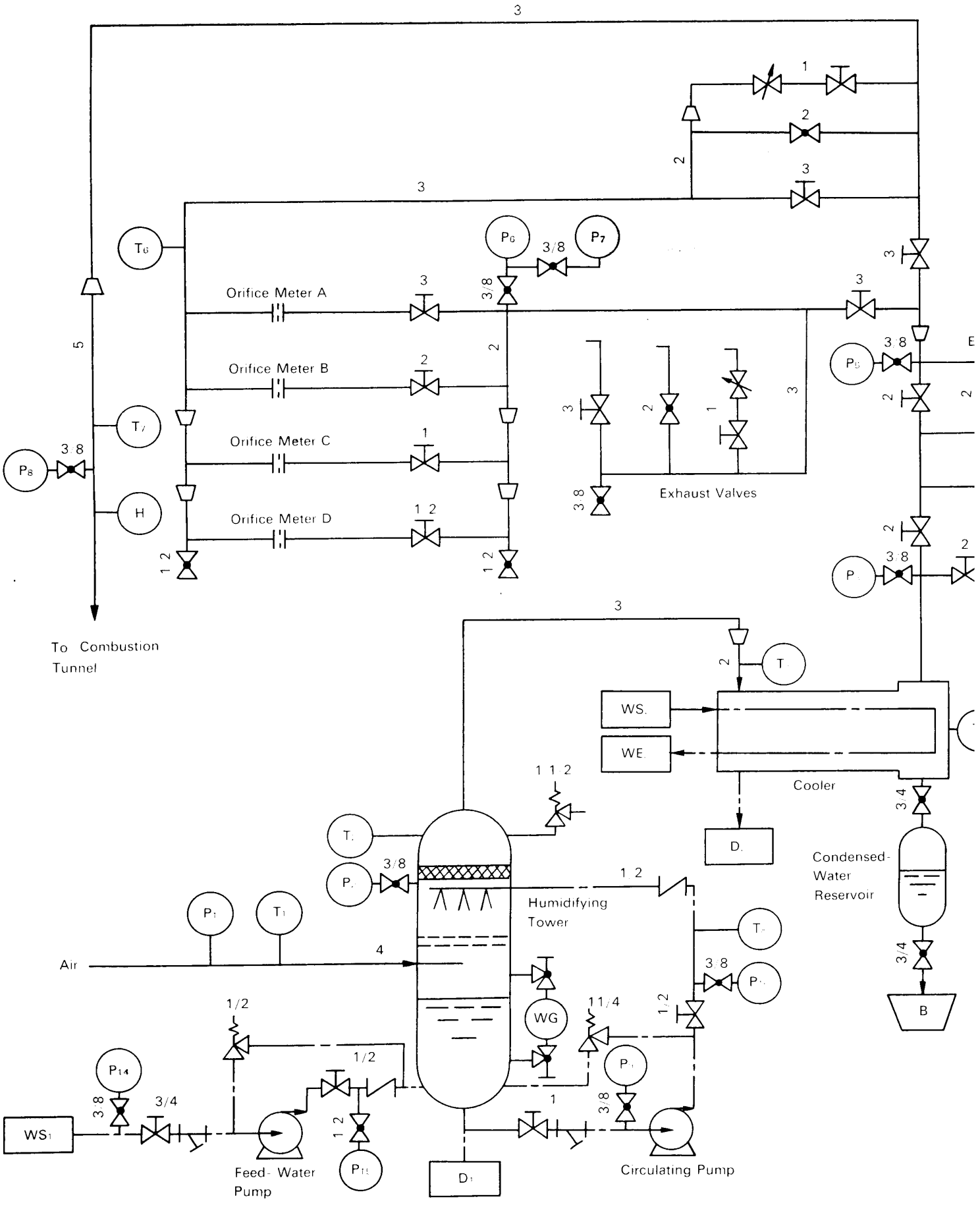

FIG. 2. Distribution diagram of the main

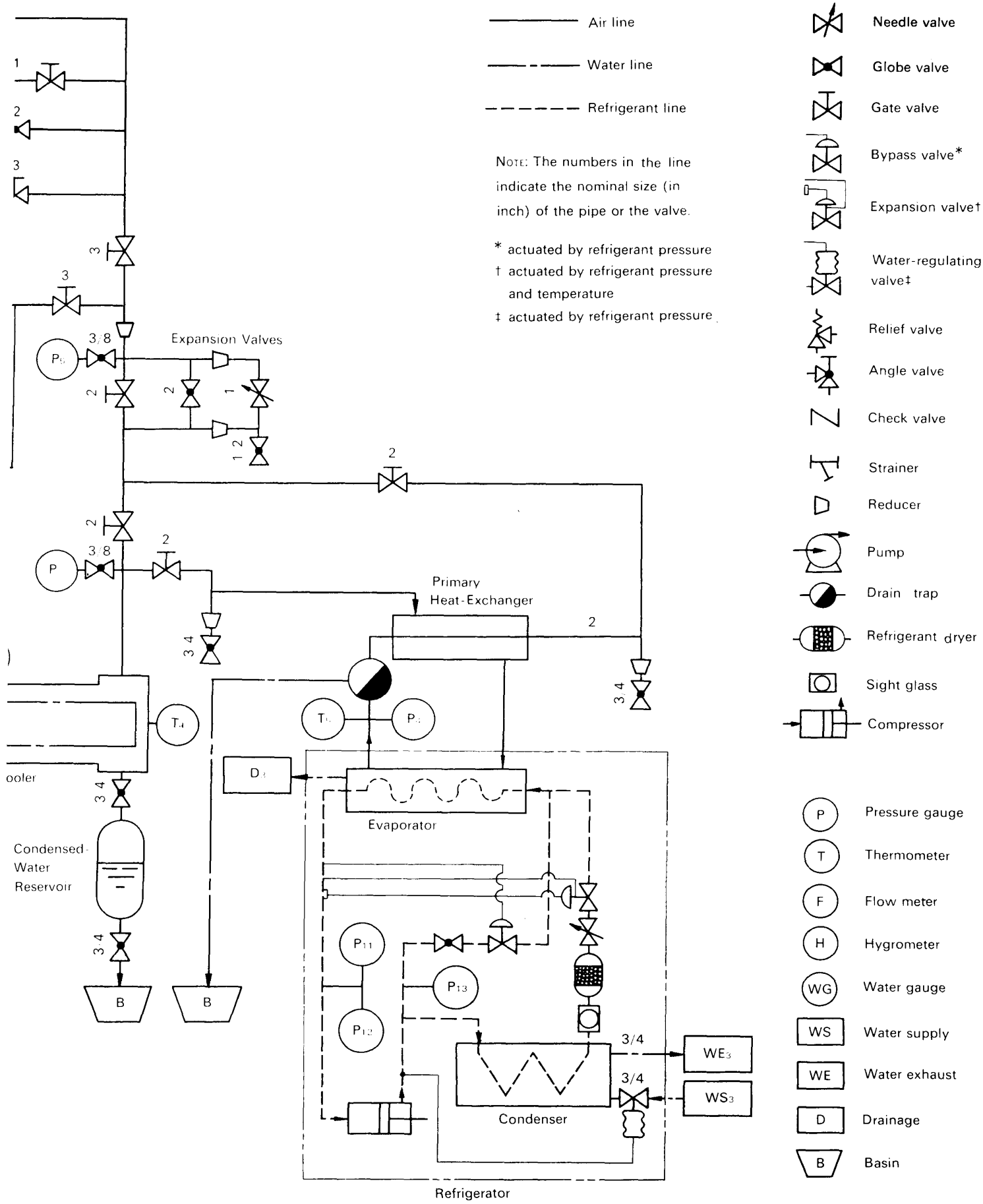

n diagram of the main lines of the system.

Table 2. SPECIFICATIONS OF AUXILIARY EQUIPMENTS

Pump

	TYPE	LIFT-HEAD MPa	CAPACITY m^3/s	DRIVING-MOTOR OUTPUT kW
Feed-Water Pump	regenerative	0.74	2.8×10^{-4}	1.5
Circulating Pump	regenerative	0.59	3.7×10^{-4}	1.5
Cooling-Water Supply Pump	two-stage centrifugal	0.29	1.5×10^{-3}	1.5

Tank

	MAXIMUM ALLOWABLE PRESSURE MPa	VOLUME m^3
Condensed-Water Reservoir	0.98	3.0×10^{-2}
Distribution Tank	0.49	3.8×10^{-1}
Overflow Tank	....	5.0×10^{-2}

temperature detected by a platinum resistance thermometer; one or both of the rest are used for base heating. The water is fed intermittently. Relevant items are as follows:

Water storage (maximum), 0.14 m^3
Controllabe range of the water temperature, room temperature $\sim$423 K
Spray pressure, 0.45 MPa
Mass flow-rate of the sprayed water, 0.44 kg/s

Cooler Figure 5 shows the structure of the cooler. It is a parallel-counterflow heat exchanger with a base heat-transfer area (the total, internal surface area of the cooling tubes) of 0.322 m^2. The controllable mass flow-rate of the cooling water ranges from 0.02 to 0.917 kg/s.

Refrigerator Figure 2 also contains the distribution diagram of the refrigerator. As is seen from the diagram, it is an ordinary, single-stage system. An alteration is that a manually-operated throttling valve is installed before the expansion valve. The flow rate of the refrigerant actually flowing into the evaporator is adjusted by this valve so that the cooling capacity can be varied (the *hot-refrigerant-bypass* method). Primary heat-exchange between the air entering the evaporator and that leaving the evaporator is made because coldness of the air leaving these dehumidifying lines is not necessary but rather harmful. Relevant items are as follows:

Refrigerant, R-12
Displacement of the compressor, 3.38×10^{-3} m^3/s
Output of the compressor-driving motor, 1.5 kW
Cooling capacity (nominal), 4.54 kW
Evaporating pressure (typical), 0.26 MPa
Condensing pressure (typical), 0.90 MPa
Heat-transfer area of the primary heat-exchanger, 1.07 m^2
Heat-transfer area of the evaporator, 13.5 m^2
Heat-transfer area of the condenser, 0.792 m^2

Table 3. Specifications of Measuring Apparatus

Thermometer

Notation	Type	Measuring Range	Minimum Scale
		°C	°C
T_1	liquid-in-glass	0～50	1
T_2	bimetal	0～150	2
T_3	liquid-in-glass	0～100	1
T_4	liquid-in-glass	0～150	2
T_5	filled-system	−10～50	0.5
T_6	liquid-in-glass	0～50	1
T_7	bimetal	0～100	2
T_8	liquid-in-glass	0～150	2
T_9	liquid-in-glass	0～50	1
T_{10}	liquid-in-glass	0～120	2
T_{11}	liquid-in-glass	0～50	1
T_{12}	liquid-in-glass	0～50	1

Pressure Gauge

Notation	Type	Measuring Range†	Minimum Scale
P_1	Bourdon-tube	0～1 MPa	0.02 MPa
P_2	Bourdon-tube	0～1.5 MPa	0.05 MPa
P_3	Bourdon-tube	0～1 MPa	0.02 MPa
P_4	Bourdon-tube	0～1 MPa	0.02 MPa
P_5	Bourdon-tube	0～1 MPa	0.02 MPa
P_6	Bourdon-tube	0～1 MPa	0.02 MPa
P_7	liquid-column (Thiesen-type)	0～4400 mmHg	1 mmHg
P_8	Diaphragm	0～3 kPa	0.1 kPa
P_9	Bourdon-tube	0～1.5 MPa	0.05 MPa
P_{10}	Bourdon-tube	0～1.5 MPa	0.05 MPa
P_{11}	Bourdon-tube	(compound)	
		−760～0 mmHg	760 mmHg
		0～15 kgf/cm^2	0.5 kgf/cm^2
P_{12}	Bourdon-tube	(compound)	
		−760～0 mmHg	200 mmHg
		0～15 kgf/cm^2	0.2 kgf/cm^2
P_{13}	Bourdon-tube	(compound)	
		−760～0 mmHg	760 mmHg
		0～25 kgf/cm^2	0.5 kgf/cm^2
P_{14}	Bourdon-tube	0～0.6 MPa	0.02 MPa
P_{15}	Bourdon-tube	0～1.5 MPa	0.05 MPa
P_{16}	Bourdon-tube	0～0.6 MPa	0.02 MPa
P_{17}	Bourdon-tube	0～1.5 MPa	0.05 MPa

Flow Meter

Notation	Type	Measuring Range	Minimum Scale
		l/min	l/min
F_1	rotameter	3～30	0.5
F_2	rotameter	1～10	0.2
F_3	rotameter	4～45	1
F_4	rotameter	3～30	0.5

Hygrometer

Notation	Type	Measuring Range	Minimum Scale
H	Electric‡	°C (dew point) −40～60	°C (dew point) 2

† in gauge pressure.

‡ Panametrics, Model 700.

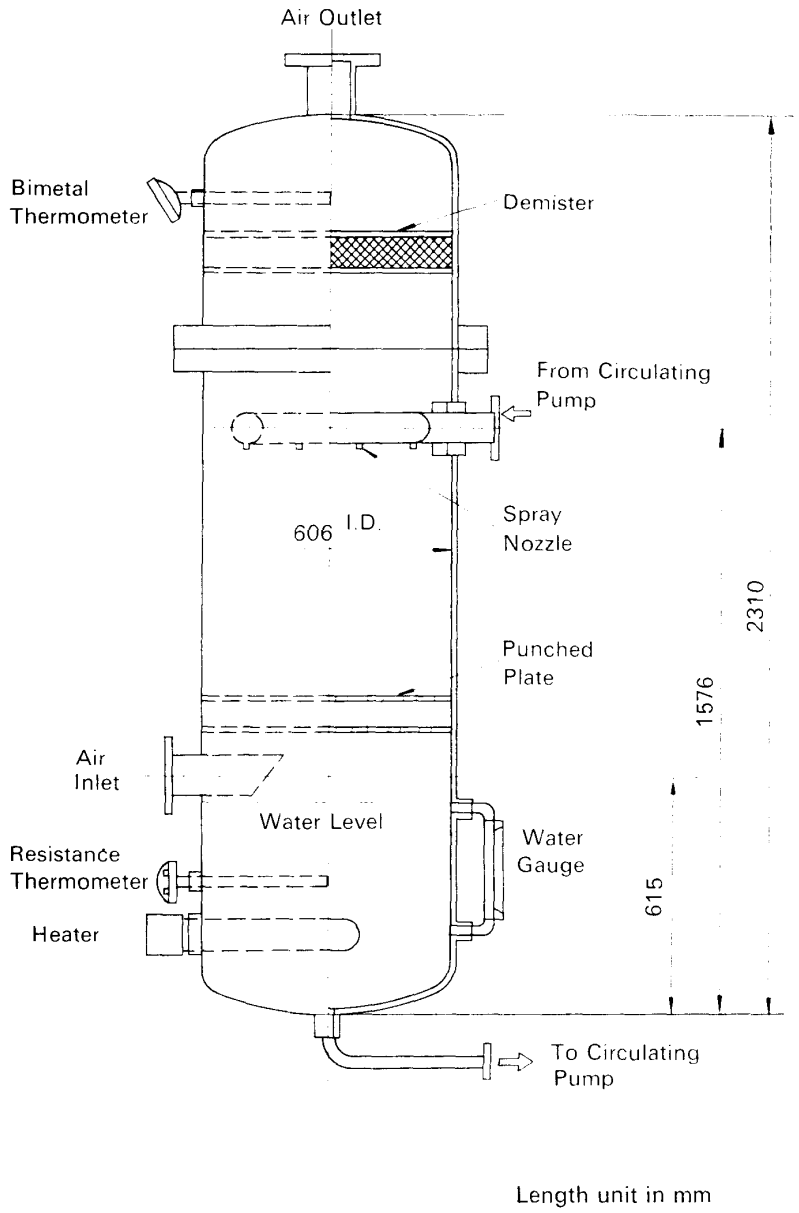

FIG. 4. Structure of the humidifying tower.

Pipe-line heater The lines to be heated are wound with electric resistors: flexible, wire resistors are used for the pipes, and flexible, ribbon-like resistors for the valves. The lines are further wrapped with a heat insulator (glass wool of 20 mm in thickness). The wall temperature of the line can be set at a desired value (room temperature $\sim$423 K) by the automatic, on-off control of the electric current of the resistors, the signal being the output of an iron-constantan thermocouple attached to the outer wall of the line. The control is made separately in seven sections; the sensing thermocouple is set in the middle part of each section. The section is illustrated in Fig. 6, and the electric power and the power density in each section are given in Table 4. The electric powers per unit surface area of the expansion-valve line and of the lines just upstream and downstream (sections I, III, and IV) are made high for compensation of reduction in the air temperature caused by expansion.

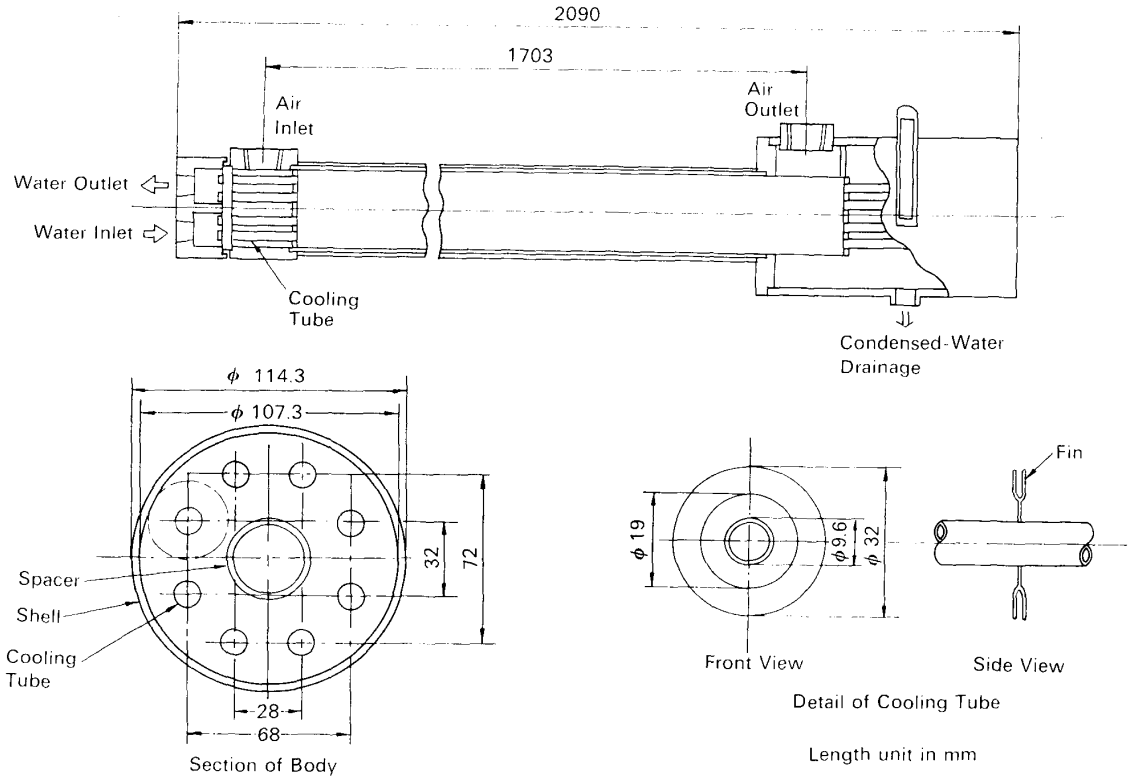

FIG. 5. Structure of the cooler.

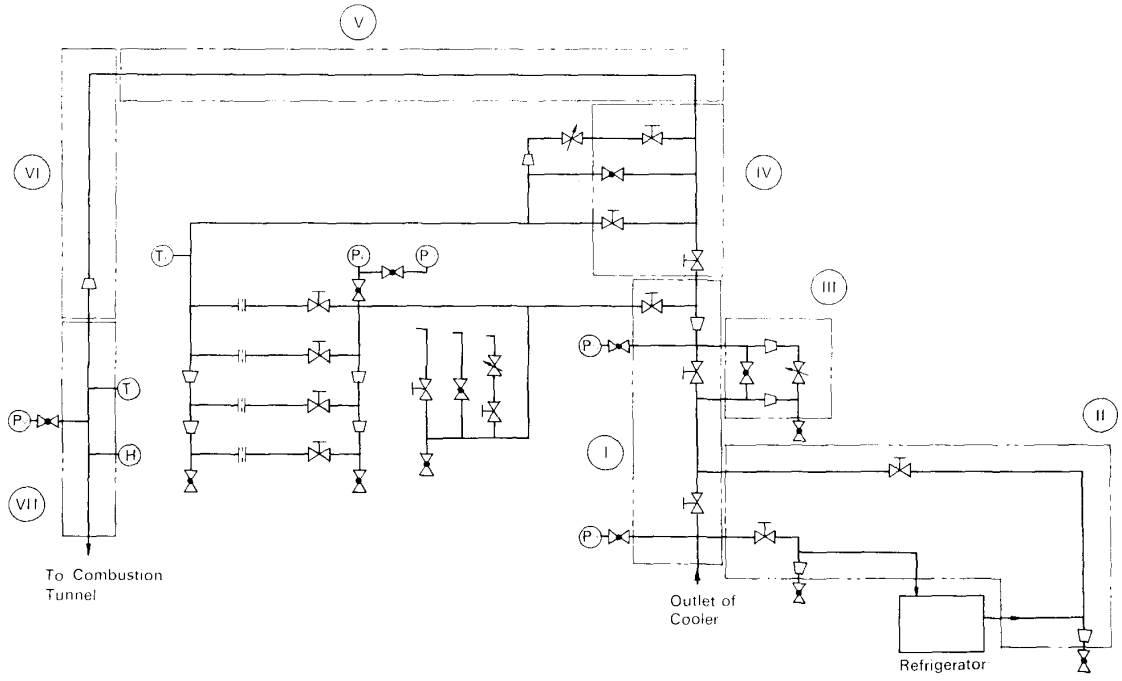

FIG. 6. Section of the pipe-line heater (cf. Fig. 2).

Table 4. Electric Power and Power Density in Each Section of Pipe-Line Heater

Notation of Division	Total Length of Line	Total Surface Area of Line	Total Electric Power	Power Per Unit Length	Power Per Unit Surface Area
	m	m^2	kW	kW/m	kW/m^2
I	1.39	0.257	3.20	2.30	12.5
II	3.96	0.632	2.62	0.662	4.15
III	2.18	0.287	3.14	1.44	10.9
IV	2.09	0.479	4.16	1.99	8.68
V	2.18	0.553	1.52	0.697	2.75
VI	2.52	0.696	1.56	0.619	2.24
VII	0.89	0.557	2.38	2.67	4.27
Total	15.21	3.461	18.58	.....	.....
Average	.....	.....	.....	1.22	5.37

Table 5. Details of Orifice Flow Meters

Notation	Inside Diameter of Pipe, D	Diameter of Orifice, d	Diameter Ratio, β $(=d/D)$	Thickness of Orifice Plate	Measurable Flow Rate† (Nominal)	
					Maximum	Minimum
	mm	mm		mm	kg/s	kg/s
A	80.7	51.0	0.632	3.0	2.21×10^{-1}	5.13×10^{-2}
B	52.9	26.4	0.499	2.0	5.58×10^{-2}	1.30×10^{-2}
C	27.6	13.6	0.493	2.0	1.47×10^{-2}	3.38×10^{-3}
D	16.1	7.0	0.435	2.0	3.85×10^{-3}	8.83×10^{-4}

† These flow rates are for a pressure upstream of the orifice of 0.12 MPa and a temperature upstream of the orifice of 293 K; the pressure reduction through the orifice is 9810 Pa for the maximum flow rate, and 490 Pa for the minimum.

Orifice flow meter Four orifice flow meters are installed in the circuit line for the control of the air flow-rate (cf. *Practice*, §2. 2). The orifices are sharp-edged, and ring taps are provided. The details of the flow meters are given in Table 5.

3. Performance of System

3.1 General Performance

Performances of the system as a whole and of the main apparatus were tested. It has been verified that the designed range of the air humidity (the dew point, 320 ~ 253 K) is covered for the air flow-rate of 0.002 ~ 0.17 kg/s. The system worked as designed without serious troubles.

3.2 Ability of the Expansion Method

The dew points of the air flow were measured with an electric hygrometer (marked H in Fig. 2 and Table 3) for various degree of expansion (including no expansion) with other experimental conditions fixed. That is, the partial pressure of water vapor

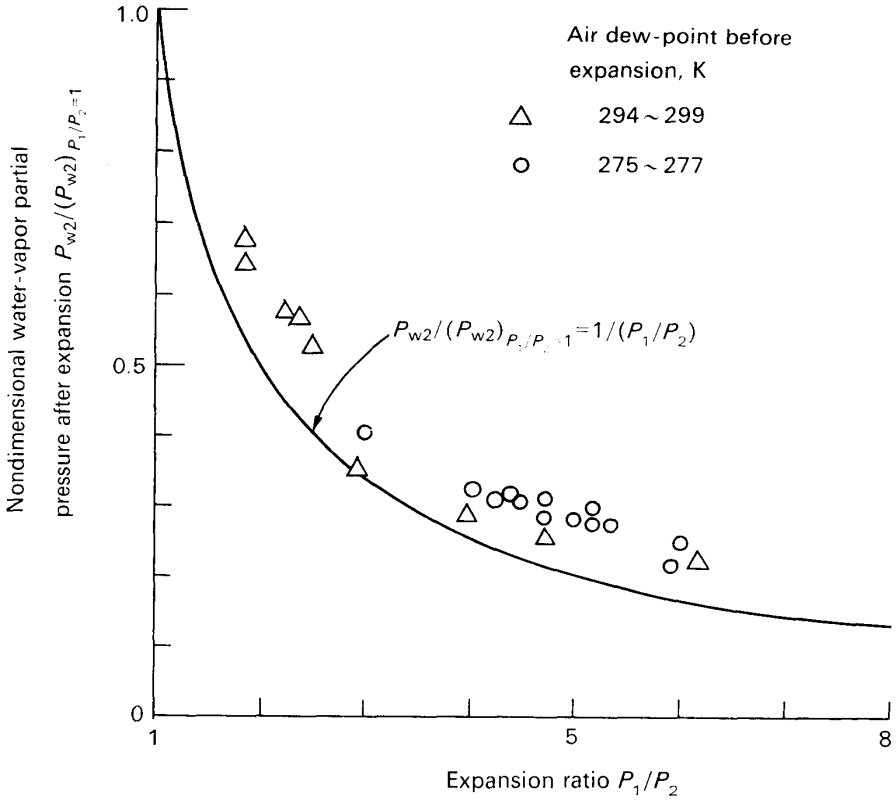

FIG. 7. Experimental results of the decrease in water-vapor partial pressure by expansion.

after expansion, P_{w2}, was measured as a function of the expansion ratio P_1/P_2. Here, P_1 is the total pressure before expansion, and P_2 after expansion. Figure 7 shows the results; in this figure, P_{w2} divided by P_{w2} for $P_1/P_2=1$ is plotted against P_1/P_2. It is seen from the figure that the nondimensional water-vapor partial pressure after expansion decreases almost hyperbolically with the expansion ratio; it is confirmed that the expansion method for decreasing air-humidity can be well put into practice. In this figure, is drawn a hyperbola representing the relation

$$P_{w2}/(P_{w2})_{P_1/P_2=1}=1/(P_1/P_2) \tag{1}$$

(cf. Eq. (A.1) in §A.1 of the Appendix). We see that this relation approximately holds here.

3.3 Performance of the Humidifying Tower

The dew points of the air at the outlet of the humidifying tower were estimated for the operation of the tower with hot-water spray (heavy humidifying) and without water spray (light humidifying). For the operation without water spray, we set the dew point at the tower outlet equal to the dew point measured with hygrometer located at the downstream end of the system, making certain that no condensation of water vapor occurs in the line between (including the cooler). For the operation with hot-water spray, we estimated the air dew-point at the tower outlet from the mass of the drainage at the cooler (i.e., the mass of water vapor condensed in the cooler) and the air dew-point downstream of the cooler, again making certain that no

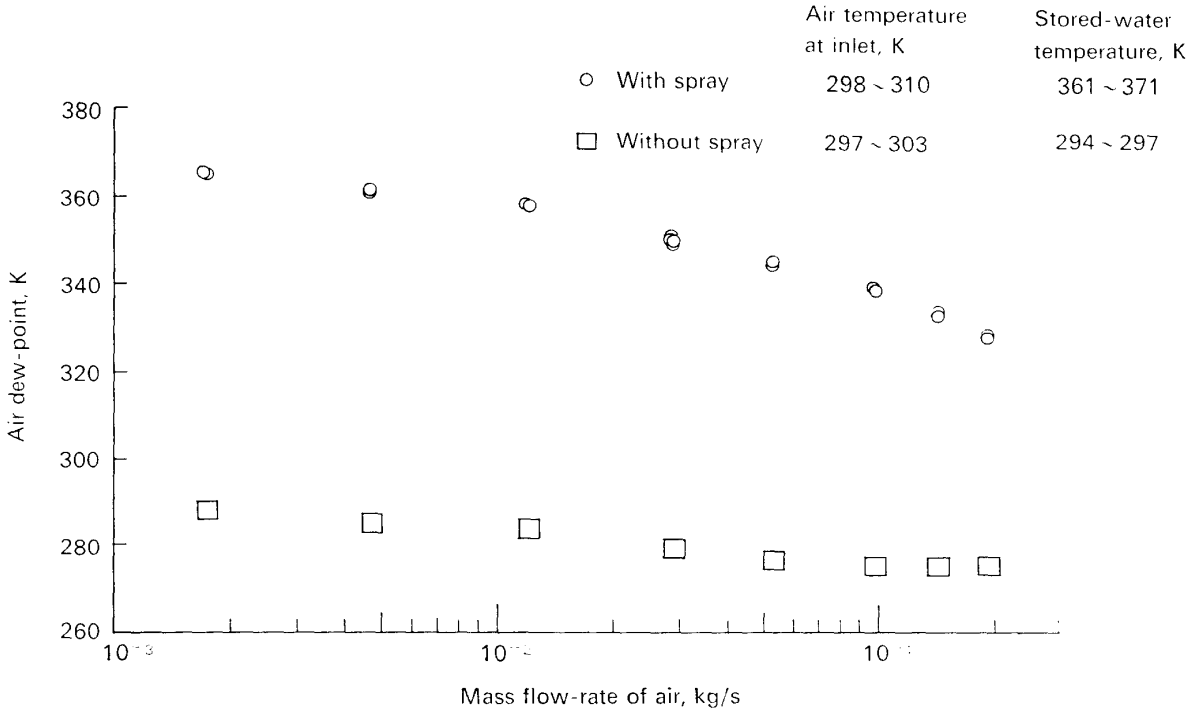

FIG. 8. Air dew-point at the outlet of the humidifying tower as a function of the mass flow-rate of the air entering the tower.

condensation of water vapor occurs in the line downstream of the outlet of the cooler.

Figure 8 shows the air dew-point at the tower outlet thus estimated as a function of the mass flow-rate of the air entering the tower (the dew point of this air is lower than 243 K). For the operation with hot-water spray, the dew point decreases gradually (first slowly, then rather sharply) with increase in the air flow-rate. But, for the operation without water spray, the air dew-point decreases slowly with the air flow-rate, and at larger air flow-rates, it remains almost unchanged. For the operation with hot-water spray, the dew point at the air mass-flow rate of 0.195 kg/s is 327 K: humidifying ability of the tower is enough for the designed maximum dew point (320 K) at the designed maximum air flow-rate (0.17 kg/s) to be reached. We can obtain different humidifying abilities by varying the temperature of the water sprayed.

Next, we arrange these results in a different way. The air dew-point at the tower outlet is transformed into relative humidity.[2] The mass flow-rate of the air entering the tower M_h is converted into the nondimensional residence time Z defined by

$$Z=\rho_h S_h \mathscr{D}/(M_h l_h). \tag{2}$$

Here, ρ_h is the density of the air in the humidifying tower; S_h the cross-sectional area of the tower; $\mathscr{D}$ the representative diffusivity; l_h the representative length. The coefficient of diffusion of water vapor in air estimated at the mean air-temperaure in the

2) The pressure and the temperature of the air at the tower outlet were also measured in the experiment.

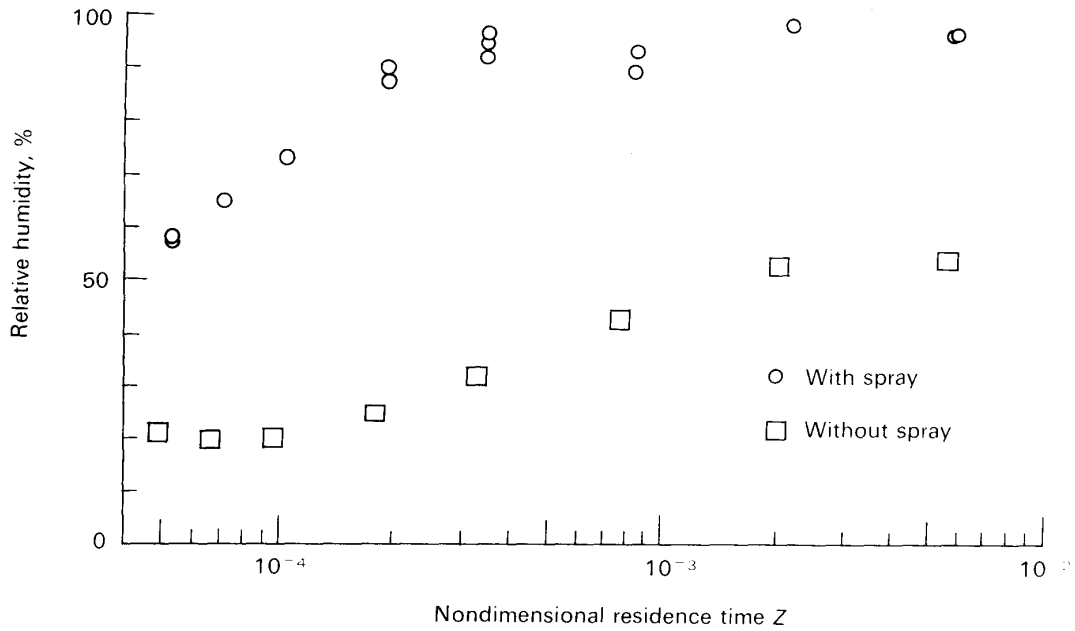

FIG. 9. Relative humidity of the air at the outlet of the humidifying tower as a function of the nondimensional residence time of the air.

tower is used as $\mathscr{D}$: $\mathscr{D}$ is taken 2.99×10^{-5} and 2.57×10^{-5} m²/s for the operation with and without water spray, respectively. The representative length l_h is conventionally taken 0.9 m, the length from the air inlet to the spray-nozzle level in the tower. The air density ρ_h is taken 1.09 and 1.18 kg/m³ for the operation with and without spray, respectively. Note that Z is essentially the reciprocal of the air mass flow-rate because ρ_h, S_h, $\mathscr{D}$, and l_h are constant.

The result of this rearrangement is shown in Fig. 9. For the operation with hot-water spray, the relative humidity first increases sharply with Z. But, as Z exceeds 3.5×10^{-4}, its behavior becomes complex: it first decreases, then increases, and again decreases. We think that this complicated behavior is caused by the complexity of the interrelation between the extent of mass transport (humidifying of the air) and that of energy transport (temperature rise of the air) in the tower. For the operation without water spray, the relative humidity first remains unchanged with Z, then increases, and again becomes unchanged. We cannot by now know why the relative humidity does not vary with Z for smaller values of Z.

3.4 Performance of the Cooler

Figure 10 shows the dew point and the temperature of the air flow at the outlet of the cooler, as a function of the flow rate of the cooling water, the air mass flow-rate being the parameter (here, the air does not pass through the refrigerator). Naturally, the dew point decreases with increase in the cooling water flow-rate, but the rate of the decrease decreases with increasing flow-rate of the cooling water. For the air flow-rate of 0.201 kg/s, the dew point varies from 326 to 311 K with the change in the cooling water flow-rate, showing that the designed maximum dew point (320 K) can be obtained for the designed maximum air flow-rate (0.17 kg/s). The range of

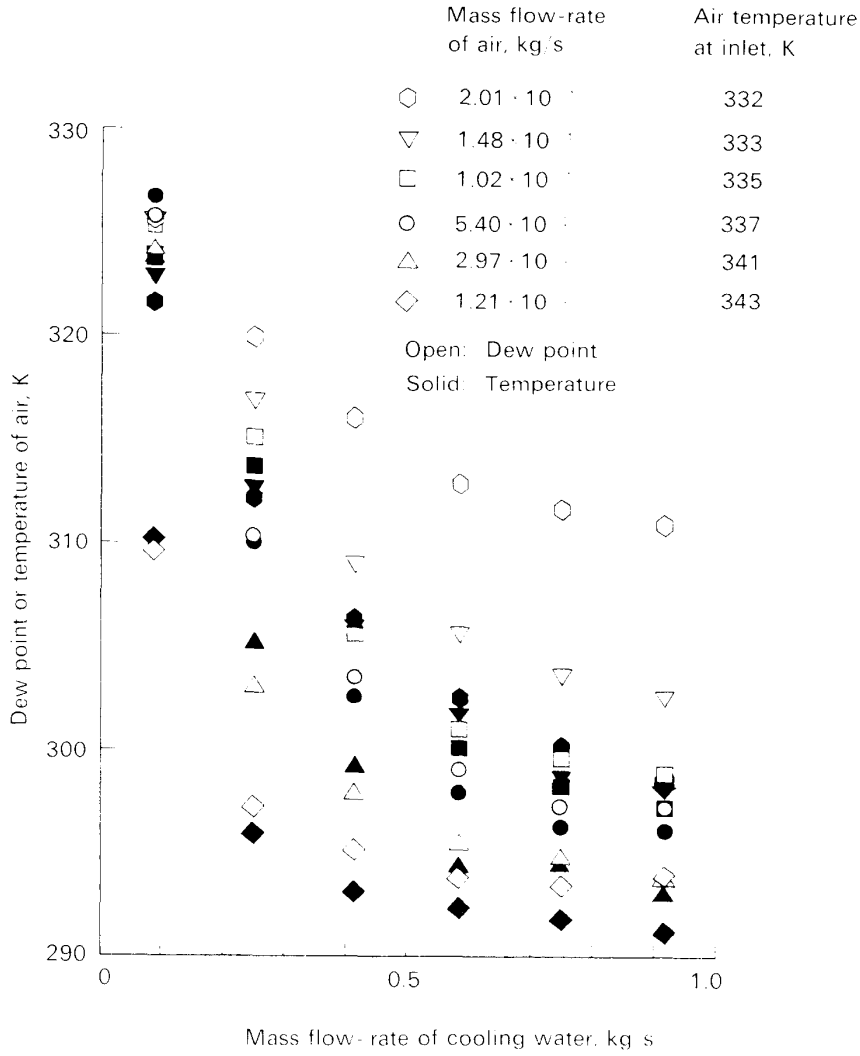

FIG. 10. Dew-point and temperature of the air at the outlet of the cooler, as a function of the mass flow-rate of the cooling water.

variation of the dew point is 15 K for the air flow-rate of 0.201 kg/s, but the ranges are wider for the smaller air flow-rates.

For the air flow-rates smaller than 0.102 kg/s, the temperature and the dew point of the air at the outlet of the cooler coincide within the error of the measuring apparatus (the thermometer, ± 1 K; the hygrometer, ± 2 K), indicating that the air is just saturated at the outlet of the cooler. But, for the air flow-rates of 0.148 and 0.201 kg/s, the dew points are higher than the temperatures. This shows that the air is supersaturated at the outlet of the cooler for these air flow-rates. This, however, does not mean that the air is still supersaturated at the exit of the system, because the air gets heated just as it leaves the cooler by the pipe-line heater. The results of the performance test of the cooler will be further analyzed in §A. 2 of the Appendix.

3.5 Performance of the Pipe-Line Heater

Figure 11 shows the rise in the air temperature through the pipe-line heater (the

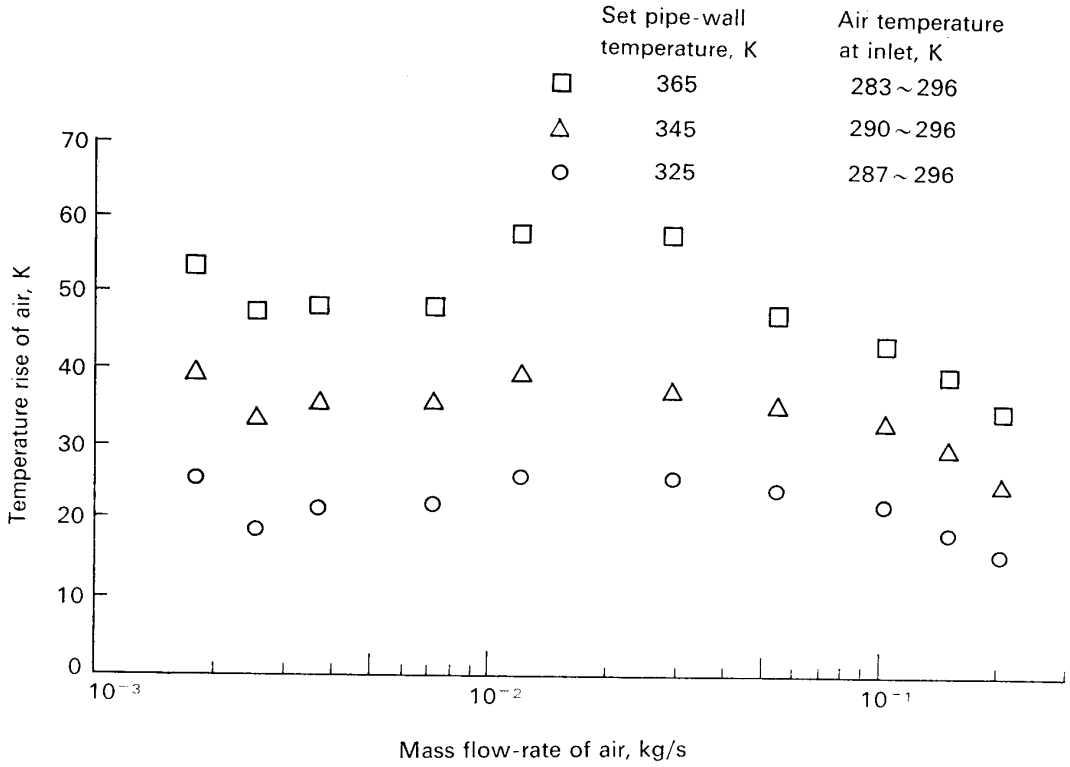

FIG. 11. Rise in the air temperature through the pipe-line heater as a function of the mass flow-rate of the air.

difference between the air temperature at the inlet of the heater and that at the outlet)[3] as a function of the mass flow-rate of the air; the parameter is the *set* pipe-wall temperature, i.e., the temperature of the wall of the pipe set by the automatic controller (in this experiment, the air not humidified is used). We see that, for all the *set* pipe-wall temperatures, the temperature rise first decreases with the air mass flow-rate, then increases, and finally again decreases; the smallest temperature rise (for the *set* pipe-wall temperature of 325 K and the air mass flow-rate of 0.206 kg/s) is 16 K. If necessary, we can raise the *set* pipe-wall temperature up to 423 K: we see that this pipe-line heater has sufficient capacity for the prevention of condensation of water vapor contained in the humid air. Reduction of these data from a heat-transfer standpoint will be made in §A. 3 of the Appendix.

3.6 *Performance of Other Apparatus and Some Points about the Operation of the System*

Refrigerator The refrigerator used is a ready-made apparatus; and it was not originally or could not afterward be fully equipped with measuring apparatus necessary for the performance tests. Therefore, we cannot make systematic tests of its performance. But, from the *condenser heat load* estimated from the temperature rise and the flow rate of the cooling water, we can infer that it has a prescribed capacity of cooling. Typical temperatures of the air at the outlet of the evaporator (measured by

3) The air does not pass through the refrigerator line in this experiment.

Table 6. EXPERIMENTALLY DETERMINED FLOW RATES FOR ORIFICE FLOW METERS

NOTATION	FLOW RATE	
	Maximum	Minimum
	kg/s	kg/s
A	2.26×10^{-1}	5.25×10^{-2}
B	5.77×10^{-2}	1.34×10^{-2}
C	1.60×10^{-2}	3.92×10^{-3}
D	3.94×10^{-3}	8.81×10^{-4}

NOTE: These flow rates are for a pressure upstream of the orifice of 0.12 MPa and a temperature upstream of the orifice of 293 K. The pressure reductions through the orifice are 9810 and 490 Pa for the maximum and the minimum flow rate, respectively. These are the same as in the last two columns of Table 5.

T5, see Fig. 2) are as follows: 270 K for the air mass flow-rate of 0.054 kg/s, 272 K for 0.13 kg/s, and 274 K for 0.17 kg/s.

Orifice flow meter The air flow-rates through the flow meters were measured by two methods. For the flow rates smaller than 1.09×10^{-3} kg/s, the wet gas meter was employed. For the larger flow rates, the flow rates were calculated from the velocity distributions at the exit of a convergent nozzle (66 mm in diameter) set downstream of the flow meters, the air velocity being measured by a pitot tube in combination with a Göttingen-type or a Chattock-type manometer.

Using these results, we have determined the product of the coefficient of discharge, the expansion factor, and the orifice area (i.e., the value necessary for the calculation of the flow rate with the knowledge of the pressure reduction and the upstream density of the fluid flowing through the orifice) for each orifice meter. Table 6 shows the maximum and the minimum flow rates calculated on the basis of the experimentally determined coefficients (these flow rates can be considered to be experimentally measured flow rates). Comparing these results with those values in the last two columns of Table 5, we find that the flow meters A and D are working as designed. But, for the flow meters B and C, the actual flow rates are smaller than the designed. Perhaps this is because manufacturing of the flow meters B and C was not accomplished exactly as designed.

Some points about the operation of the system There are some points which we noticed while actually operating the present system. These we describe here for information.

1. When the final control of the air dew-point is made at the cooler by the regulation of the cooling water flow-rate, a fluctuation of the flow rate (even a small one) causes a similar fluctuation of the air dew-point: one must supply cooling water with little fluctuation of the flow rate, if one wants to control accurately the air dew-point by a cooler.[4)]

2. Control of the air dew-point in a wide range by a commercially available refrigerator is difficult because such refrigerators are usually made so that their cooling

4) At first, we fed city water directly into the cooler. But we could not control accurately the air dew-point because of the flow-rate fluctuation; we were compelled to feed the cooling water by a pump in combination with an overflow tank.

capacity remains as unchanged as possible under varied conditions: one must specially design a refrigerator in which the cooling capacity can widely be changed if one wants to control the air dew-point in a wide range by a refrigerator.

3. In the present system, when the air flow-rate is large and the air dew-point is high, supply of water to the humidifying tower and drainage of the condensed water from the cooler must be done frequently (both of them are now handworked and really troublesome): these should be done automatically for larger systems.

4. Water vapor adsorbs tenaciously at the walls of the lines, and it takes surprisingly much time for the system to be dried down to a low dew-point level: one must wait patiently the attainment of equilibrium in the system when one wants to use air of a low dew-point.

4. Concluding Remarks

The present system has been working as designed without troubles: this system could make an example of a variably-humidified air flow supplying system of a laboratory scale. One point we want to emphasize last is that the method for decreasing air humidity by expansion is effective and also easy to be practiced.

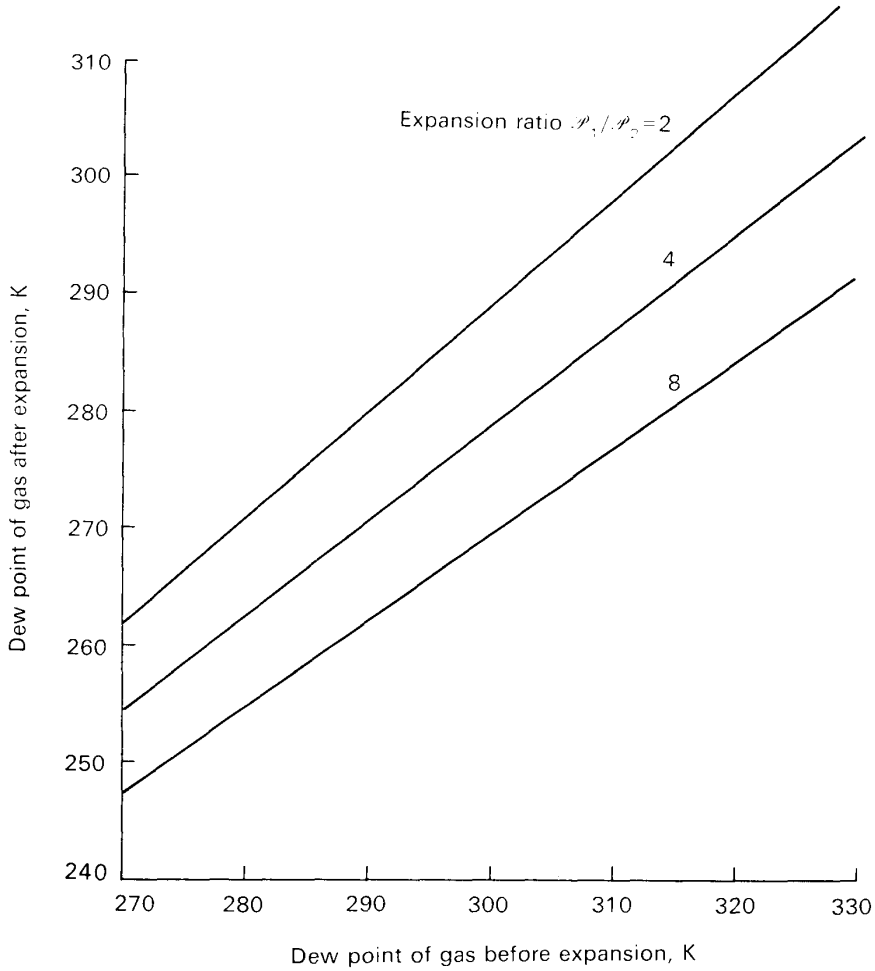

Fig. 12. Decrease in the dew point of a gas by expansion.

APPENDIX

A.1 Explanation of the Expansion Method

If a humid gas of the total pressure $\mathscr{P}_1$ and the water-vapor partial pressure $\mathscr{P}_{w1}$ expands to a state of the total pressure $\mathscr{P}_2$ with neither addition nor extraction of water vapor, then the water-vapor partial pressure after expansion, $\mathscr{P}_{w2}$, is given by

$$\mathscr{P}_{w2}=\mathscr{P}_{w1}\mathscr{P}_2/\mathscr{P}_1. \tag{A.1}$$

That is, the water-vapor partial pressure, therefore the dew point, of a humid gas decreases by expansion. (In the present discussion, supersaturation or undercooling of the gas is excluded.) We can best illustrate this decrease by expressing the water-vapor partial pressure of a humid gas in terms of its dew-point and representing in a diagram the dew point after expansion as a function of the dew point before expansion, with the expansion ratio taken parameter. Figure 12 is such a diagram. We see that the dew point of a humid gas much decreases when the expansion ratio is large.

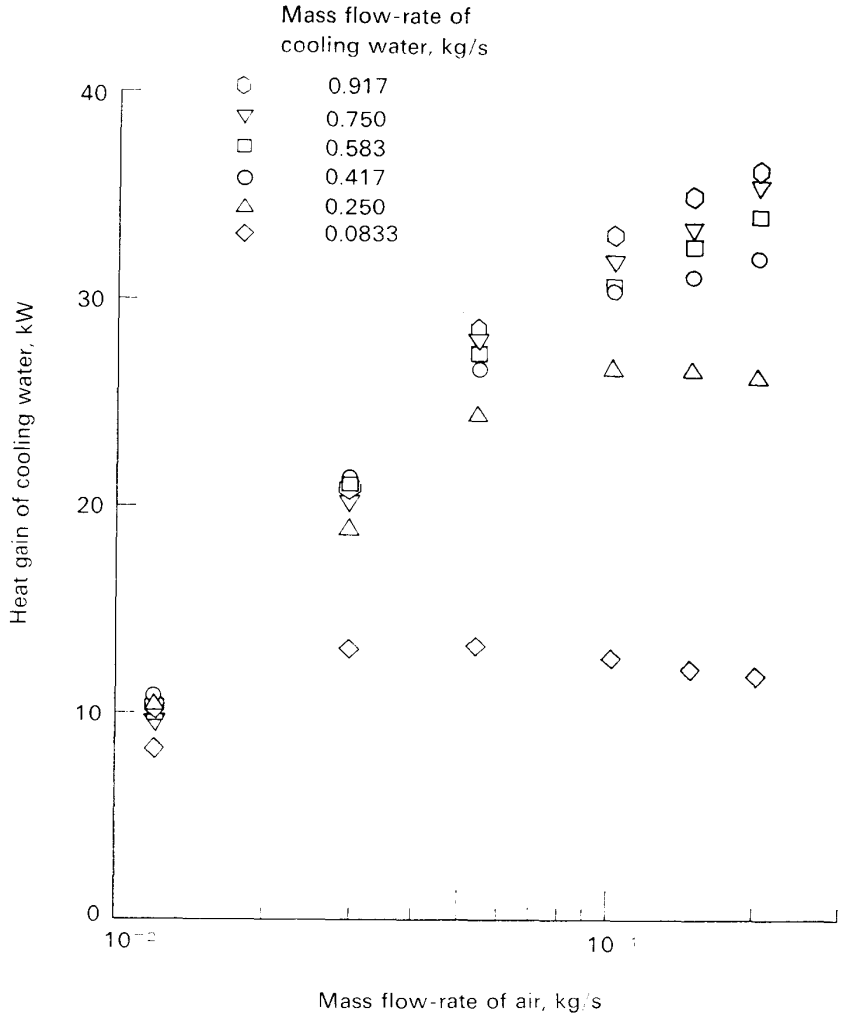

FIG. 13. Heat gain of the cooling water as a function of the mass flow-rate of the air; the temperature of the air at the cooler inlet ranges from 332 to 343 K.

A.2 Further Analysis of the Test Results of the Cooler

Figure 13 shows the relation between the heat gain of the cooling water (cf. Eq. (A.2)) and the mass flow-rate of the air (excluding the mass of water vapor contained in it). For the cooling water flow-rates of 0.0833 and 0.250 kg/s, the heat gain first increases and then decreases with increasing air flow-rate. This will be due to the decrease in the difference between the temperature of the humid air and that of the cooling water for the larger air flow-rates. For the larger flow-rates of the cooling water, the heat gain increases monotonically with the air flow-rate.

We can deduce the rate of heat transfer from the humid air to the cooling tube by making some assumptions. We assume first that the heat gain of the cooling water is equal to the heat loss of the humid air. We think this assumption reasonable because the heat loss from the casing of the cooler to the surrounding atmosphere is small. On this assumption the heat loss of the humid air Q is given by

$$Q=c_{\mathrm{w}}(T_{\mathrm{w}2}-T_{\mathrm{w}1})w. \tag{A.2}$$

Here, $T_{\mathrm{w}1}$ and $T_{\mathrm{w}2}$ are the temperature of the cooling water at the inlet and at the outlet of the cooler, respectively; c_{w} is the specific heat of the water, and w the mass flow-rate of the cooling water. The overall heat-transfer coefficient U is defined by

$$U=\frac{Q}{(T_{\mathrm{a}}-T_{\mathrm{w}})_{\mathrm{mn}}A}, \tag{A.3}$$

where $(T_{\mathrm{a}}-T_{\mathrm{w}})_{\mathrm{mn}}$ is the mean temperature difference, and A the heat-transfer area. The mean temperature difference appropriate for the parallel-counterflow heat exchanger is

$$(T_{\mathrm{a}}-T_{\mathrm{w}})_{\mathrm{mn}}=\frac{\sqrt{(T_{\mathrm{a}1}-T_{\mathrm{a}2})^2+(T_{\mathrm{w}2}-T_{\mathrm{w}1})^2}}{\ln\left[\dfrac{(T_{\mathrm{a}1}+T_{\mathrm{a}2})-(T_{\mathrm{w}1}+T_{\mathrm{w}2})+\sqrt{(T_{\mathrm{a}1}-T_{\mathrm{a}2})^2+(T_{\mathrm{w}2}-T_{\mathrm{w}1})^2}}{(T_{\mathrm{a}1}+T_{\mathrm{a}2})-(T_{\mathrm{w}1}+T_{\mathrm{w}2})-\sqrt{(T_{\mathrm{a}1}-T_{\mathrm{a}2})^2+(T_{\mathrm{w}2}-T_{\mathrm{w}1})^2}}\right]}, \tag{A.4}$$

in which $T_{\mathrm{a}1}$ is the temperature of the humid air at the inlet of the cooler, and $T_{\mathrm{a}2}$ that at the outlet [2]. In the present configuration, the cooling water flows inside the circular tube, and the humid air outside. Therefore, the overall heat-transfer coefficient is expressed by

$$1/U=1/h_{\mathrm{a}}+b/k+1/h_{\mathrm{w}}. \tag{A.5}$$

In this expression h_{a} is the heat-transfer coefficient for the air side, h_{w} for the water side, b the thickness of the tube, and k the thermal conductivity of the tube material.

We assume next that h_{w} is proportional to the 0.8 power of w.[5] Then, we can write as

$$1/U=1/h_{\mathrm{a}}+b/k+1/(aw^{0.8}) \tag{A.6}$$

(a is a constant). We assume third that h_{a} is a function of the mass flow-rate of the humid air only. Then, for a given mass flow-rate of the humid air, the relation

$$1/U=\text{constant}+1/(aw^{0.8}) \tag{A.7}$$

5) It is well known that this relation really holds when the temperature of the tube wall is constant and the Reynolds number of the fluid flowing in the tube is larger than 20,000 [3].

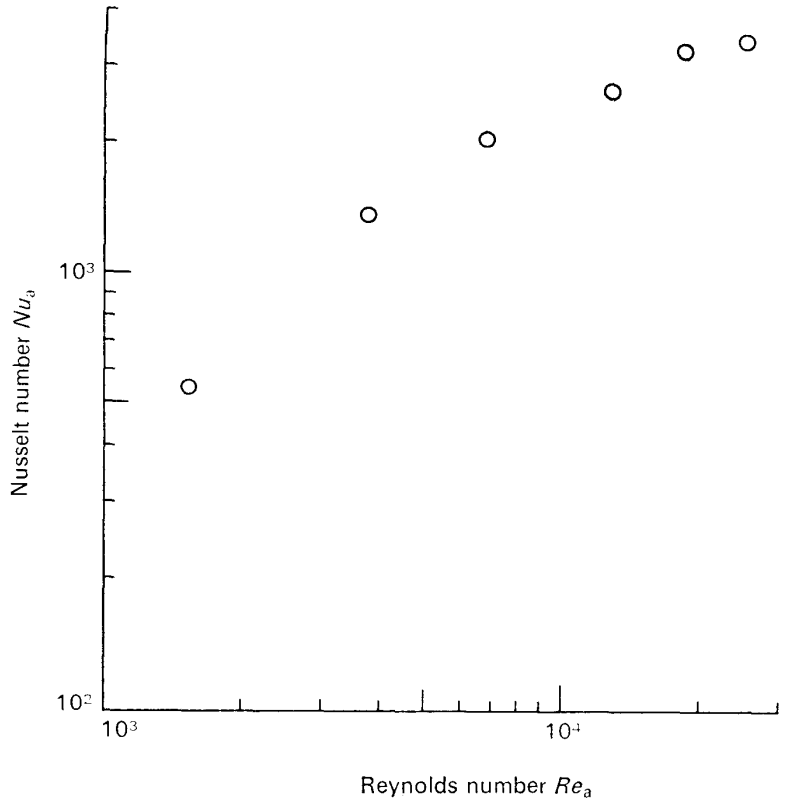

FIG. 14. Nusselt number for heat transfer (humid-air side) as a function of the Reynolds number of the humid-air flow.

holds because b/k is originally invariable. So, if $1/U$ is plotted against $1/w^{0.8}$ for a given mass flow-rate of the humid air, the value of the ordinate at the origin gives $1/h_a+b/k$ for that flow rate of the humid air. From this we obtain $1/h_a$ because we can calculate b/k from the knowledge of the size and the material of the cooling tube.[6]

The heat-transfer coefficient h_a thus obtained is expressed in the form of the Nusselt number Nu_a $(=h_a l_a/k_a)$ with the representative length l_a taken equal to the external diameter of the cooling tube (9.6 mm) and the thermal conductivity k_a equal to 2.89×10^{-2} W/(m·K) [4]. The mass flow-rate of the humid air M_a is converted into the Reynolds number Re_a by the relation

$$Re_a = M_a l_a/(S_a \mu_a)\,, \tag{A.8}$$

where S_a and μ_a are the cross-sectional area of air-passage in the cooler and the kinematic viscosity of the humid air, respectively. We set $S_a=7.56\times 10^{-3}$ m^2 and $\mu_a=$ 12.8 μPa·s (the value for the humid air saturated at 343 K). The relation between Nu_a and Re_a is shown in Fig. 14. We see that Nu_a increases monotonically with Re_a. The rate of increase in Nu_a with Re_a decreases with increase in Re_a.

A.3 Further Analysis of the Test Results of the Pipe-Line Heater

In the pipe-line heater used in this system, the air is heated by flowing inside the lines whose walls are kept at a nearly constant temperature. This situation is similar

6) The material of the tube is copper ($k=0.35$ kW/(m·K)) and the thickness of the tube is 0.8 mm; therefore, b/k is 2.3×10^{-3} m^{2}K/kW, which can be neglected in actual calculation of $1/h_a$.

to that of a simple heater in which a fluid flowing inside a straight circular tube with a constant wall temperature is heated.[7] Therefore, we reduce the result shown in Fig. 11 in the similar way as is successfully taken in treating heat transfer in such a heater [3, 5].

The rise in the fluid temperature through the heater is converted into so called the Colburn j factor for heat transfer; and this factor is expressed as a function of the Reynolds number of the fluid flow. The Colburn j factor, here denoted by j, is defined by

$$j=St_f Pr_f^{2/3}\left(\frac{\mu_o}{\mu_b}\right)^{0.14}=Nu_f Re_f^{-1}Pr_f^{-1/3}\left(\frac{\mu_o}{\mu_b}\right)^{0.14}, \tag{A.9}$$

where St_f is the Stanton number ($=Nu_f Re_f^{-1}Pr_f^{-1}$), Nu_f the Nusselt number, Pr_f the Prandtl number, and μ the kinematic viscosity of the fluid; the subscripts b and o mean that the kinematic viscosity is evaluated at the bulk temperature and at the wall temperature, respectively. As the temperature difference, necessary for calculation of the heat-transfer coefficient on which the Nusselt number is evaluated, we take the logarithmic mean temperature difference

$$(T_s-T_f)_{ln}=\frac{[(T_{s1}-T_{f1})-(T_{s2}-T_{f2})]}{\ln[(T_{s1}-T_{f1})/(T_{s2}-T_{f2})]}, \tag{A.10}$$

where T_f is the temperature of the fluid, and T_s the wall; the subscripts 1 and 2 indicate the temperature at the inlet and at the outlet of the heater, respectively. Therewith, the j factor is expressed more specifically as

$$j=\frac{T_{f2}-T_{f1}}{(T_s-T_f)_{ln}}\left(\frac{D_p}{4L_p}\right)\left(\frac{\mu_b c_{pb}}{k_b}\right)^{2/3}\left(\frac{\mu_o}{\mu_b}\right)^{0.14}. \tag{A.11}$$

In this expression, c_{pb} and k_b are the specific heat at constant pressure and the thermal conductivity of the fluid (both evaluated at the bulk temperature), respectively; D_p is the (inside) diameter and L_p the length of the tube.

Our experimental results (Fig. 11) rearranged in this way are shown in Fig. 15. Here, the bulk temperature (the temperature at which μ_b, c_{pb}, and k_b are evaluated) is taken $(T_{f1}+T_{f2})/2$; the wall temperature is taken the *set* pipe-wall temperature ($T_{s1}=T_{s2}$ in this heater). The Reynolds number Re_f is given by $D_p G_f/\mu_b$, G_f being the mass velocity of the air flow; D_p is 0.0807 m, and L_p 7.26 m ($L_p/D_p=90.0$). It is seen in Fig. 15 that the differences in the *set* pipe-wall temperatures are cancelled and the j factor varies simply as a function of Re_f. We see that this way of data reduction is effective here. The j factor first decreases with Re_f, then increases slightly, and finally again decreases.

In Fig. 15 is drawn a line evaluated by the following, widely accepted relations proposed for heating (cooling) of a fluid flowing in a circular tube with a constant wall-temperature:

$$j=1.86Re_f^{-2/3}(D_p/L_p)^{1/3} \text{ (Sieder and Tate [3]) for } Re_f<2{,}200, \tag{A.12}$$

$$=0.116(Re_f^{2/3}-125)Re_f^{-1}[1+(D_p/L_p)^{2/3}] \text{ (Hausen [5])} \tag{A.13}$$

7) The differences are that, in the present heater, the line does not simply consist of a circular tube (it contains valves) and is not throughout straight (it contains some right-angled bends).

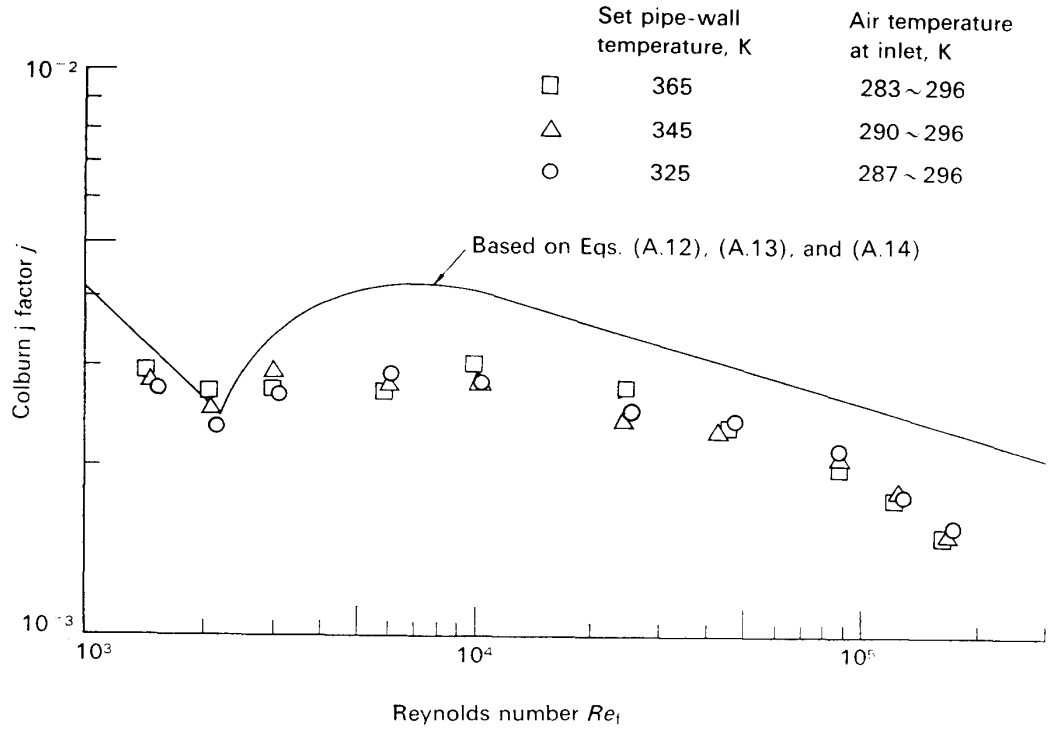

FIG. 15. The Colburn j factor for heat transfer as a function of the Reynolds number of the air flow.

$$\text{for } 2{,}200 \leq Re_f \leq 9{,}800,$$

$$= 0.026 Re_f^{-0.2} \text{ (Sieder and Tate [3]) for } Re_f > 9{,}800. \qquad \text{(A.14)}$$

We see that the experimental variation of the j factor with Re_f is generally akin to the variation of the line; especially, for $Re_f \leq 2{,}200$ the experimental points lie close to the line. For $Re_f > 2{,}200$ the experimental j factors are smaller than those of the line. Perhaps this is because in our experiment the wall temperature is, on the average, smaller than the *set* pipe-wall temperature. In fact, the lines are rather coarsely wound by the electric resistors.

ACKNOWLEDGEMENT

We acknowledge the financial support of the Grant-in-Aid for Scientific Research (B) of the Ministry of Education, Subject No. 246058 (1977 and 1978). The main part of the present system was manufactured by Mikuni Kikai Kogyo Co., Ltd., and the pipe-line heater by Tôyô Dennetsu Co., Ltd. We are grateful to Messrs. M. Tamaoka and H. Imaizumi of the Mikuni Kikai and Mr. N. Nomura of the Tôyô Dennetsu for their efforts and advice. We also thank Mr. M. Kokufuda for his co-operation in making performance tests and data reduction.

Department of Jet Propulsion
Institute of Space and Aeronautical Science
University of Tokyo
19 December 1979

References

[1] Tsuji, H., Hori, M., Okano, T., and Yamaoka, I., "On the Variable Pressure Combustion Tunnel," Bull. Inst. Space and Aero. Sci., Univ. of Tokyo **1**, 475–498 (1965) [in Japanese].

[2] Giedt, W. H., *Principles of Engineering Heat Transfer* (D. Van Nostrand Co., Inc., Princeton, 1957) pp. 339–346.

[3] Bird, R. B., Stewart, W. E., and Lightfoot, E. N., *Transport Phenomena* (John Wiley & Sons, Inc., New York, 1960) pp. 396–407.

[4] Grüß, H., and Schmick, H., "Über die Wärmeleitfähigkeit von Gasgemischen," Wissensch. Veröff. Siemens Konzern **7**, 202–224 (1928).

[5] Perry, R. H., and Chilton, C. H., *Chemical Engineers' Handbook* (McGraw-Hill Book Co., New York, 1973) 5th ed., Sect. 10, pp. 12–16.

Notation

The section and the equation to be referred to are given in brackets. The unit in SI is added for information.

A heat-transfer area of cooler [§A.2, Eq. (A.3)], m^2

a constant appearing in the expression of h_w [§A.2, Eqs. (A.6) and (A.7)], $J/(m^2 \cdot kg^{0.8} \cdot s^{0.2} \cdot K)$ $(=kg^{0.2}s^{-2.2}K^{-1})$

b thickness of cooling tube [§A.2, Eqs. (A.5) and (A.6)], m

c_w specific heat of cooling water [§A.2, Eq. (A.2)], $J/(kg \cdot K)$ $(=m^2s^{-2}K^{-1})$

c_{pb} specific heat at constant pressure of fluid evaluated at the bulk temperature [§A.3, Eq. (A.11)], $J/(kg \cdot K)$ $(=m^2s^{-2}K^{-1})$

D inside diameter of pipe [Table 5], m

D_p inside diameter of tube [§A.3, Eqs. (A.11)$\sim$(A.13)], m

$\mathscr{D}$ representative diffusivity [§3.3, Eq. (2)], m^2/s

d diameter of orifice [Table 5], m

G_f mass velocity of fluid [§A.3], $kg/(m^2 \cdot s)$

h_a heat-transfer coefficient for air side [§A.2, Eqs. (A.5) and (A.6)], $W/(m^2 \cdot K)$ $(=kg \cdot s^{-3}K^{-1})$

h_w heat-transfer coefficient for water side [§A.2, Eq. (A.5)], $W/(m^2 \cdot K)$ $(=kg \cdot s^{-3}K^{-1})$

j Colburn j factor [§A.3, Eqs. (A.9), (A.11)$\sim$(A.14)], nondimensional

k thermal conductivity of cooling-tube material [§A.2, Eqs. (A.5) and (A.6)], $W/(m \cdot K)$ $(=m \cdot kg \cdot s^{-3}K^{-1})$

k_a thermal conductivity of humid air [§A.2], $W/(m \cdot K)$ $(=m \cdot kg \cdot s^{-3}K^{-1})$

k_b thermal conductivity of fluid evaluated at the bulk temperature [§A.3, Eq. (A.11)], $W/(m \cdot K)$ $(=m \cdot kg \cdot s^{-3}K^{-1})$

L_p length of tube [§A.3, Eqs. (A.11)$\sim$(A.13)], m

l_a representative length [§A.2, Eq. (A.8)], m

l_h representative length [§3.3, Eq. (2)], m

M_a mass flow-rate of humid air [§A.2, Eq. (A.8)], kg/s

M_h mass flow-rate of air entering humidifying tower [§3.3, Eq. (2)], kg/s

Nu_a Nusselt number of humid air [§A.2], nondimensional

Nu_f Nusselt number of fluid [§A.3, Eq. (A.9)], nondimensional

P_1 total pressure of humid air before expansion [§3.2, Eq. (1)], Pa $(=m^{-1}kg \cdot s^{-2})$

P_2 total pressure of humid air after expansion [§3.2, Eq. (1)], Pa ($=m^{-1}kg\cdot s^{-2}$)

P_{w2} water-vapor partial pressure of humid air after expansion [§3.2, Eq. (1)], Pa ($=m^{-1}kg\cdot s^{-2}$)

$\mathscr{P}_1$ total pressure of gas before expansion [§A.1, Eq. (A.1)], Pa ($=m^{-1}kg\cdot s^{-2}$)

$\mathscr{P}_2$ total pressure of gas after expansion [§A.1, Eq. (A.1)], Pa ($=m^{-1}kg\cdot s^{-2}$)

$\mathscr{P}_{w1}$ water-vapor partial pressure of gas before expansion [§A.1, Eq. (A.1)], Pa ($=m^{-1}kg\cdot s^{-2}$)

$\mathscr{P}_{w2}$ water-vapor partial pressure of gas after expansion [§A.1, Eq. (A.1)], Pa ($=m^{-1}kg\cdot s^{-2}$)

Pr_f Prandtl number of fluid [§A.3, Eq. (A.9)], nondimensional

Q heat loss of humid air [§A.2, Eqs. (A.2) and (A.3)], W ($=m^2kg\cdot s^{-3}$)

Re_a Reynolds number of humid air [§A.2, Eq. (A.8)], nondimensional

Re_f Reynolds number of fluid [§A.3, Eqs. (A.9), (A.12)~(A.14)], nondimensional

S_a cross-sectional area of air-passage in cooler [§A.2, Eq. (A.8)], m^2

S_h cross-sectional area of humidifying tower [§3.3, Eq. (2)], m^2

St_f Stanton number of fluid [§A.3, Eq. (A.9)], nondimensional

T_{a1} temperature of humid air at the inlet of cooler [§A.2, Eq. (A.4)], K

T_{a2} temperature of humid air at the outlet of cooler [§A.2, Eq. (A.4)], K

T_{f1} temperature of fluid at the inlet of heater [§A.3, Eqs. (A.10) and (A.11)], K

T_{f2} temperature of fluid at the outlet of heater [§A.3, Eqs. (A.10) and (A.11)], K

T_{s1} wall temperature at the inlet of heater [§A.3, Eq. (A.10)], K

T_{s2} wall temperature at the outlet of heater [§A.3, Eq. (A.10)], K

T_{w1} temperature of cooling water at the inlet of cooler [§A.2, Eqs. (A.2) and (A.4)], K

T_{w2} temperature of cooling water at the outlet of cooler [§A.2, Eqs. (A.2) and (A.4)], K

$(T_a-T_w)_{mn}$ mean temperature difference [§A.2, Eqs. (A.3) and (A.4)], K

$(T_s-T_f)_{ln}$ mean temperature difference [§A.3, Eqs. (A.10) and (A.11)], K

U overall heat-transfer coefficient [§A.2, Eqs. (A.3), (A.5)~(A.7)], $W/(m^2\cdot K)$ ($=kg\cdot s^{-3}K^{-1}$)

w mass flow-rate of cooling water [§A.2, Eq. (A.2)], kg/s

Z nondimensional residence time [§3.3, Eq. (2)], nondimensional

β diameter ratio [Table 5], nondimensional

μ_a kinematic viscosity of humid air [§A.2, Eq. (A.8)], Pa·s ($=m^{-1}kg\cdot s^{-1}$)

μ_b kinematic viscosity of fluid evaluated at the bulk temperature [§A.3, Eqs. (A.9) and (A.11)], Pa·s ($=m^{-1}kg\cdot s^{-1}$)

μ_o kinematic viscosity of fluid evaluated at the wall temperature [§A.3, Eqs. (A.9) and (A.11)], Pa·s ($=m^{-1}\,kg\cdot s^{-1}$)

ρ_h density of air in humidifying tower [§3.3, Eq. (2)], kg/m^3